SECURITY INFORMATION

CONFIDENTIAL

Copy 6
RM E53H19

UNCLASSIFIED

NACA RM E53H19

NACA

RESEARCH MEMORANDUM

INVESTIGATION AT MACH NUMBERS 1.5 AND 1.7 OF TWIN-DUCT SIDE INTAKE SYSTEM WITH TWO-DIMENSIONAL 6° COMPRESSION RAMPS MOUNTED ON A SUPERSONIC AIRPLANE

By Joseph Davids and George A. Wise

Lewis Flight Propulsion Laboratory
Cleveland, Ohio

CLASSIFICATION CHANGED

To UNCLASSIFIED

By authority of _____ Date _____

CLASSIFIED DOCUMENT

This material contains information affecting the National Defense of the United States within the meaning of the espionage laws, Title 18, U.S.C., Secs. 793 and 794, the transmission or revelation of which in any manner to an unauthorized person is prohibited by law.

NATIONAL ADVISORY COMMITTEE
FOR AERONAUTICS

WASHINGTON

October 12, 1953

CONFIDENTIAL

UNCLASSIFIED

UNCLASSIFIED

NASA Technical Library
3 1176 01435 2802

NACA RM E53H19

NATIONAL ADVISORY COMMITTEE FOR AERONAUTICS

RESEARCH MEMORANDUM

INVESTIGATION AT MACH NUMBERS 1.5 AND 1.7 OF TWIN-DUCT SIDE INTAKE SYSTEM WITH TWO-DIMENSIONAL 6° COMPRESSION RAMPS MOUNTED ON A SUPERSONIC AIRPLANE

By Joseph Davids and George A. Wise

SUMMARY

An experimental investigation was conducted in the Lewis 8- by 6-foot supersonic wind tunnel to determine the performance characteristics of a twin-duct side intake system joining into a common duct and utilizing two-dimensional 6° compression ramps mounted on a supersonic airplane at Mach numbers of 1.5 and 1.7. Tests were made for several inlet configurations at various angles of attack, angles of yaw, and mass-flow ratios. The configurations were investigated to determine the effects of (1) ramp-support struts, (2) side fairings, (3) blunt and sharp cowl lips, and (4) a revised area distribution in the subsonic diffuser.

All the configurations investigated resulted in small changes in inlet performance characteristics. It was found that, at low mass-flow ratios, one inlet would operate at a higher mass-flow ratio than the other for all the tests. Lowering the inlet so that part of the ramp was immersed in the boundary layer decreased appreciably the subcritical mass-flow range in which both ducts would operate at the same mass-flow conditions.

Increasing the rate of expansion in the subsonic diffuser for the blunt-lip inlet without side fairings increased the critical-pressure recovery approximately $1\frac{1}{2}$ percent at a Mach number of 1.5.

INTRODUCTION

The performance of a particular inlet is dependent upon the flow field in which it is immersed. If the flow field is uniform, it is possible to determine the performance characteristics theoretically; but if the flow is distorted, the complexity of the problem is greatly increased. In particular, if the inlet is mounted on the side of some arbitrary fuselage, the behavior of the inlet with respect to such

CONFIDENTIAL

UNCLASSIFIED

variables as location, degree of boundary-layer removal, orientation of the fuselage, and shape of the fuselage must be experimentally determined. Therefore, an investigation was conducted to determine the internal performance and drag characteristics of a twin-duct intake system mounted on the sides of a supersonic airplane fuselage. The inlets utilized a 6° two-dimensional compression ramp, and, during the course of the investigation, several modifications to the inlets and a modifed duct-area variation were tested.

The investigation was conducted in the Lewis 8- by 6-foot supersonic wind tunnel at Mach numbers of 1.5 and 1.7 through a range of angles of attack and engine mass-flow ratios. The Reynolds number of the investigation was approximately 14.5×10^6 based on the length of the fuselage ahead of the inlet.

2976

SYMBOLS

The following symbols are used in this report:

A	area
A_i	projected frontal area of inlet (including projected ramp area), sq ft
C_D	model external drag coefficient based on maximum frontal cross-sectional area of 2.097 sq ft, $\frac{D}{q_0 A_f}$
D	drag
h	height of boundary-layer ram scoop
L	length of subsonic diffuser, 74.0 in.
M	Mach number
$\frac{m}{m_0}$	engine mass-flow ratio, $\frac{\rho_3 V_3 A_3}{\rho_0 V_0 A_i}$
P	total pressure
p	static pressure
q	dynamic pressure, $\frac{\gamma p M^2}{2}$
V	velocity
x	distance from cowl lip, model station 36.00

[redacted]

α model angle of attack, deg

β flow deflection with respect to inlet center line, deg

γ ratio of specific heats, 1.40

δ boundary-layer thickness

ρ mass density of air

Subscripts:

av average

c model station 110.00

f frontal

i inlet

0 free stream

1 fuselage survey station, model station 31.00

2 diffuser-inlet survey station, model station 37.50

3 diffuser-exit survey station, model station 102.105

Pertinent areas:

A_f maximum frontal cross-sectional area, 2.097 sq ft

A_3 duct area at diffuser-discharge station, 0.326 sq ft

APPARATUS AND PROCEDURE

Twin-duct, ramp-type side inlets were mounted symmetrically on the fuselage forebody of a one-fourth scale model of a supersonic airplane (fig. 1). The model was sting mounted from a tunnel strut with an internal strain-gage balance connecting the model to the sting. A shroud, also connected to the sting, covered the various drive mechanisms and formed a continuation to the fuselage. Two reverse scoops, located near the top of the shroud, were used to lower the pressure at the base of the model. The shroud was mounted entirely independently of the model and was believed to have no appreciable effect on the external drag.

2976

CQ-1 back

A drawing of the basic configuration with representative model cross sections is presented in figure 2. The nose of the model and the inlets were canted down at an angle of 5° with respect to the main fuselage axis, and, as a result, the inlets were in line with the free-stream direction when the body was at an angle of attack of 5°. Mass flows through the inlets and boundary-layer ducts were varied by means of remotely controlled plugs attached to the model sting.

The inlets consisted of nearly rectangular-shaped cowls with 6° two-dimensional compression ramps. The twin main ducts were geometrically similar and joined into a common duct at model station 101.25. Duct cross section, which was nearly rectangular at the inlet, changed gradually to an annular cross section at the junction.

2976

Ram-type boundary-layer passages were located beneath each inlet ramp to remove the fuselage boundary-layer air. These passages, which discharged parallel to the main duct, were rectangular in cross section at the inlet with a gradual change to a circular cross section at the exit. Boundary-layer air in excess of that taken in through the passages was deflected by wedges as shown in figure 3.

Sections of the inlet configurations tested are shown in figure 2, and details are shown in figure 3. To facilitate discussion of the various inlets, the following notation system is used hereinafter:

Designation	Description
B	Blunt lip
S	Sharp lip
F	Side fairings
NF	No side fairings
A	Modified duct-area variation

The B-F configuration was the initial inlet tested, and all comparisons made in this report are with respect to this inlet unless otherwise stated. Included in the program were configuration changes to determine the effect of ramp-support struts, the effect of lowering the inlet so that part of the ramp was immersed in the boundary layer, and the effect of removing the inlet side fairings.

The very gradual rate of expansion in the subsonic diffuser, by maintaining a higher Mach number for a longer distance, indicated high friction losses. Since it was thought possible that expansion in the high Mach number region could decrease the subsonic diffuser losses, inlet B-NF was modified to include a more rapid expansion in the subsonic diffuser (fig. 4). To obtain the modified rate of expansion, it was

necessary to raise the ramps, thereby decreasing the inlet area. This, in turn, caused a small increase in the projected area of the boundary-layer passage as shown in detail B of figure 3. The aforementioned configurations with sharpened cowl lips were also investigated. Details of the sharp lips are shown in figures 3(b) and (e) and detail A.

All the configurations tested, including those for which no data are presented, and some pertinent measurements are as follows:

2976

Inlet tested	Projected inlet frontal area, A_i, sq ft	Boundary-layer bleed height (at center of inlet), h, in.	$\frac{h}{\delta}$
B-F	0.263	0.4	≥ 1.0
B-NF	.263	.3	≥ 1.0
B-F with ramp struts	.263	.3	≥ 1.0
B-F	.256	.2	< 1.0
B-NF-A	.238	.3	≥ 1.0
S-F	.256	.3	≥ 1.0
S-NF	.256	.3	≥ 1.0

Photographs of the various inlet configurations are presented in figure 5.

Instrumentation in one of the main ducts included three inlet rakes of five tubes each, located at model station 37.50. A static-pressure orifice was located at the base of each rake. These rakes were used to calculate, by an area weighting method, the average total pressures at the entrance to the subsonic diffuser. When the rakes were installed, similar dummy rakes were installed in the other duct to obtain symmetrical flow. The exit of the diffuser, model station 102.105, was instrumented with twelve wall static orifices and six radial rakes equally spaced. Each rake consisted of four total-pressure tubes located at the centers of equal areas. Four wall static orifices were located at model station 110.00 in the main duct and were used in the mass-flow calculations. Static-pressure orifices were located near the junction of the two ducts (model station 74.00) and pressure-sensitive pickups were used to detect flow instability. The rear bulkhead was instrumented with six static-pressure orifices which were used to calculate the base forces. A survey of local Mach number and flow deflection upstream of one of the inlets was obtained with the use of two 6° half-angle wedge bars. Schematic diagrams of the wedge bars and their locations as well as a summary of the results of the survey are shown in figure 6. The local Mach numbers

and flow deflections presented are arithmetic averages of the four measured values. An additional survey in front of one of the inlets at model station 31.00 was conducted to determine the thickness of the boundary layer and the total-pressure losses ahead of the inlet. The survey was made with three rakes of eight tubes each, and the results at an angle of attack of 5° are presented in figure 7. The profiles showed a negligible change with angle of attack for the range of the investigation. Boundary-layer thickness was determined from the profiles, and the local Mach numbers obtained from the wedge survey were used to correct the measured total pressures for normal shock recovery in order to determine the losses ahead of the inlet.

2976

The force-measuring system consisted of an internal strain-gage balance located at a forward model station and a strain-gage link mounted between the sting and the rear model bulkhead. The rear link was mounted so as to measure only a normal force component without influencing the axial force. In addition to measuring a normal force, the rear link restrained the model in pitch, thereby eliminating most of the model deflection due to imposed air loads. The balance and strain-gage link measured the combined internal duct forces, fuselage drag, and model base forces, but did not measure the forces acting on the mass-flow-control plugs. The drag presented is the streamwise component of the external forces, excluding the base pressure forces due to the difference in base pressure from free-stream static pressure and stream thrust developed by the main-duct flow from free stream to exit. Included in drag is the momentum change due to the flow through the boundary-layer ducts. From data not presented, however, the boundary-layer-duct force was found to be negligible and probably did not affect the accuracy of the drags presented.

Body angle of attack was measured with an internal angle-of-attack indicator; the same indicator was used to measure angle of yaw when the fuselage was rotated 90° about its axis.

The mass flows through the twin main ducts were calculated from the known open area at the exit and the average of the static pressures at station 110.00 with the assumption that the flow was choked at the geometrical minimum area of the exit. The diffuser total-pressure recoveries at survey station 3 upstream of the rake were computed from the calculated mass flows and the average static pressure at station 3.

Mass-flow ratio m/m_0 is defined as the ratio of the mass flow through the diffuser ducts to that flowing in the free stream through an area equal to the total inlet projected area. The mass-flow ratios calculated are considered to be accurate to ±2 percent and the total-pressure recoveries to within ±1 percent.

The investigation was conducted at free-stream Mach numbers of 1.5 and 1.7; model angles of attack of 0°, 1.5°, 5°, 9.5°, and -2.8°; and model angles of yaw of 0°, 3°, and 6° for a range of mass-flow ratios. The Reynolds number based on the length of the fuselage ahead of the inlets was approximately 14.5×10^6.

RESULTS AND DISCUSSION

Figure 8 presents the performance characteristics of the B-F inlet at Mach numbers 1.5 and 1.7 for a range of angles of attack. Also shown are lines of constant diffuser-exit Mach number M_3. For both Mach numbers, peak pressure recovery occurred at an angle of attack of 5°, at which angle the inlets and the forebody were in line with the free-stream direction. For this configuration at a Mach number of 1.5, the diffuser performance was relatively insensitive to angles of attack greater than 5° but was reduced at angles of attack less than 5°. With decreasing mass-flow ratio, diffuser total-pressure recovery increased at a Mach number of 1.5 and decreased slightly at a Mach number of 1.7. The theoretical supercritical mass-flow ratio computed from the geometry of the inlet at a Mach number of 1.5 is $2\frac{1}{2}$ percent greater than that obtained experimentally. This difference is probably due to a curvature of the ramp oblique shock as compared with the theoretical straight shock. Cross-plotted data not presented for this and other configurations indicate that minimum drag was obtained between angles of attack of 1.5° and 5°. The drag rise from critical remained the same over the entire range of angle of attack for both Mach numbers.

To support the ramp, struts were added between the ramp and the fuselage, and an investigation was made to determine their effect on inlet performance. Data not presented indicate that the critical-pressure recovery decreased on the order of 1 percent with lower recoveries over the entire subcritical region. This decrease is probably due to the effect on the fuselage boundary layer associated with the ramp struts, which extended ahead of the ramp leading edge. Had the struts been swept rearward from the leading edge of the ramp, it is probable that the effect of the struts on inlet performance could have been reduced.

The height of the ramp from the fuselage for inlet B-F was such that no boundary-layer air was taken aboard the inlet. In order to determine the effect on inlet performance of incomplete boundary-layer removal, the B-F configuration was tested with the ramp closer to the fuselage. Because of the curvature of the fuselage, only the center portion of the ramp was immersed in boundary-layer air. Data not presented indicate that, even though only a small region of the inlet was directly affected by the boundary layer, critical-pressure recovery

decreased 1 percent and the mass-flow range in which the twin inlets operate at their maximum pressure recovery decreased appreciably. At slightly reduced mass-flow ratios in the region of 0.850, one inlet captured considerably less mass flow than the other. This condition can be attributed in part to differences in the flow separation off the ramps of the two inlets and will be discussed later in greater detail.

Performance curves for the B-NF configuration are shown in figure 9 for Mach numbers 1.5 and 1.7. In comparison with the B-F inlet, the effect of removing the side fairings on diffuser pressure recovery can be seen to be negligible and within the accuracy of the data. It can be noted, however, that at mass-flow ratios below 0.8, pressure recovery decreased slightly as compared with the B-F inlet. Increases in drag coefficient can be seen at both Mach numbers. At Mach number 1.5, a slight increase in drag coefficient can be seen at all angles of attack except 5°. However, at Mach number 1.7, the increase in drag coefficient is larger and occurs at both angles of attack of 1.5° and 5°. This drag increase is believed to be caused in part by the difference in inlet external fairing that results with the removal of side fairings.

Figure 10 presents the inlet total-pressure contours for one duct of inlet B-NF at angles of attack of 1.5° and 5° for several mass-flow ratios. It can be seen at a Mach number of 1.5 that, for a mass-flow ratio near critical and at an angle of attack of 5°, a relatively large region of high-pressure air exists over the face of the inlet with regions of low-energy air at the corners of the inlet. At reduced mass-flow ratios, the ramp boundary layer thickens as indicated by the larger region of low-energy air and ultimately results in flow separation off the ramp. It can be noted that, for a near critical mass-flow ratio, a larger area of low-energy air exists at an angle of attack of 1.5° than at an angle of attack of 5°. At a Mach number of 1.7, the contours at mass flows less than critical indicate that a region of reverse flow occurred as a result of separation at angles of attack of 1.5° and 5°.

Schlieren photographs presented in figure 11 verify the presence of separation as seen in the inlet contours for both Mach numbers. It can also be noted that the curvature of the oblique shock occurs near the ramp as mentioned previously. These schlieren photographs were taken with the model in the yaw position at an angle of yaw of zero; and, because the nose and model inlets were canted 5° with respect to the fuselage center line, the inlet angle of attack is -5° with respect to the free-stream direction.

Total-pressure contours at station 3 are shown in figure 12(a) to (c) at Mach number 1.5 for mass-flow conditions comparable to those presented in figure 10. The right side of the duct of figure 12 (as the reader sees it) is in line with the inlet for which the total-pressure contours

9762

are presented. From figure 12(a) and (b) for high subcritical mass-flow ratio, a symmetrical flow pattern exists in the duct, with the high-pressure region equally distributed on the sides of the duct in line with the inlets. From this distribution it is evident that both ducts are operating at the same mass-flow conditions for both angles of attack. With decreasing mass flow at an angle of attack of 5° (fig. 12(c)), asymmetry results with one side of the duct operating at a higher total-pressure level than the other. In this particular case, the right side of the duct captures less mass flow than the left. This asymmetric flow condition probably is a function of the differences in separation off the ramps of the two inlets. The separation at reduced mass-flow ratios is shown in figure 10. It must be mentioned that, though these contours of figure 12 indicate the left duct to be operating at a higher mass-flow ratio than the right, both ducts experienced this condition at some time during the test. For these conditions, the inlet shock system exhibited no tendency to oscillate periodically.

Figure 12(d) presents a contour showing a condition where one duct operated supercritically while the other operated with reverse flow. For all the configurations tested, at very low mass-flow ratios, one duct operated supercritically while the other operated with almost completely reverse flow. Two factors that may determine which duct operates supercritically are minor differences in the construction of the two inlets and asymmetry in the flow entering the inlets.

A breakdown of the total-pressure losses for the B-NF configuration at Mach numbers 1.5 and 1.7 at an angle of attack of 5° is shown in figure 13. The total-pressure loss ahead of the inlet was computed from an integration of the total pressures measured with total-pressure rakes ahead of the inlet and was found to be essentially the same at both Mach numbers. The supersonic losses were calculated using the integrated total pressures at the inlet rake station 37.50, and the ducting or subsonic diffuser losses were obtained using the integrated total pressures at the exit rake station 102.105. Also included in the figure are estimated supersonic and subsonic diffuser total-pressure losses. Included in these estimations are the experimental pressure losses ahead of the inlet. The supersonic losses were calculated from the shock configuration, which consisted of one oblique and one normal shock. For the subsonic diffuser, losses of 6.7 percent of free-stream total pressure at Mach number 1.5 and 5.7 percent of free-stream total pressure at Mach number 1.7 were estimated from an adaptation of the method of reference 1. These losses were estimated for critical conditions only. The experimental results at a Mach number of 1.5 showed the supersonic losses to remain relatively constant with reduced mass-flow ratio to around 0.8 and to increase thereafter. The increase at reduced mass flows can be attributed to increasing amounts of separation off the ramps (and/or the separated flow not reattaching to the duct surface).

2976 CQ-2

The estimated supersonic loss at critical mass flow is approximately 2 percent less than the experimental values, probably caused in part by corner effects as shown in figure 10(a) to 10(c). The large ducting loss at a critical mass-flow ratio of 0.95 for Mach number 1.5 can be attributed to the high subsonic inlet Mach number and the slow rate of expansion existing in the initial portion of the subsonic diffuser. These factors are examined later. With decreasing mass flow, the ducting loss can be seen to decrease. The decreasing ducting loss, along with the essentially constant supersonic losses to a mass-flow ratio of 0.8, accounts for the increase in pressure recovery seen in figure 9(a). The supersonic losses increased at a faster rate than the subsonic losses decreased at mass-flow ratios below 0.8, accounting for the decrease in total-pressure recovery also seen in figure 9(a). At Mach number 1.7 the experimental supersonic losses are somewhat higher than estimated as a result of a relatively thick ramp boundary layer and corner effects shown in figure 10(d) to 10(f). The supersonic losses increase with decreasing mass-flow ratio, partly because of ramp separation and reverse flow, also shown in figure 10. At reduced mass-flow ratios, a vortex sheet can be seen to enter the inlet as shown in figure 11(d). The lower energy air outside this vortex sheet entering the inlet would also necessarily increase the supersonic total-pressure loss.

2976

The rate of diffusion in the initial portion of the subsonic diffuser was very low, as shown in figure 4. This low rate of diffusion tended to maintain the high subsonic Mach number that existed at the entrance of the diffuser at a free-stream Mach number of 1.5 and resulted in relatively high friction losses. Therefore, in an effort to reduce friction losses at Mach number 1.5, the area distribution in the subsonic diffuser of inlet B-NF was modified so as to attain an increased rate of expansion near the inlet. The inlet ramp was raised to attain the area variation; the resulting modification of the external configuration caused a small increase in the boundary-layer-system frontal area as shown in figure 3. Therefore, any comparison of drag coefficient is invalid because of the configuration change. Figure 14 presents the performance results of the modification to inlet B-NF (designated as inlet B-NF-A). Critical-pressure recovery at angles of attack of 5° and 9.5° increased $1\frac{1}{2}$ percent as compared with inlet B-NF (fig. 9(a)) at Mach number 1.5. At Mach number 1.7 the pressure recovery was essentially the same within the accuracy of the data. It was to be expected that the performance at a Mach number of 1.7 would not be improved as much as at a Mach number of 1.5, since the inlet Mach number was lower than at 1.5; the decrease in friction losses therefore would be less significant.

Performance at angles of yaw of 0°, 3°, and 6°, together with total-pressure contours, is presented in figure 15 at Mach number 1.5 for inlet B-NF-A. At a body angle of yaw of zero, the inlets are at an angle of attack of -5° with respect to the free-stream direction because of the

5° droop of the nose and inlets. With increasing angle of yaw, peak pressure recovery decreased rapidly, whereas the supercritical mass-flow ratio remained relatively constant. The total-pressure contours are presented for angles of yaw of 3° and 6° for a supercritical and subcritical mass-flow ratio. At angles of yaw of 3° and 6° for a critical mass-flow ratio of 0.885, a somewhat larger high-pressure region exists in the windward duct than in the leeward duct, as would be expected. With reduced mass-flow ratio, this condition becomes more pronounced. The performance of the windward duct would necessarily be higher, since at angle of yaw the Mach number ahead of the inlet is lower as a result of compression by the fuselage; the effective ramp angle is larger, decreasing the possibility of shock-induced separation; and the boundary layer is thinner. The leeward duct would experience a thicker boundary layer and a higher inlet Mach number.

The internal contraction associated with a blunt-lip inlet could increase the inlet Mach number and subsequently the subsonic-diffuser losses. Also, the possibility of obtaining higher cowl pressure drags at supersonic speeds would tend to increase the over-all drag of the configuration investigated. In order to eliminate the internal contraction and to evaluate the effect on the accompanying high ducting losses, particularly at Mach number 1.5, the cowl lips of inlet B-F and B-NF were sharpened and investigated. The variations of diffuser total-pressure recovery and drag coefficient with mass-flow ratio are shown in figure 16 for inlet S-F. Results of the investigation indicate no appreciable change in performance as compared with inlet B-F, and, therefore, the effect of contraction due to the blunt lip appeared to be negligible. A slight increase in drag coefficient can be noted, but can be attributed probably to the change in inlet external fairing aft of the cowl lip caused by the sharpening of the lip. Data not presented show the removal of side fairings to have no effect on the inlet performance.

With the exception of the performance characteristics of inlet B-NF-A, all the modifications to the B-F inlet investigated had little or no effect on internal performance. It can be concluded that, for the model and the variables investigated, the designer has a relatively large freedom of choice in his selection of an inlet configuration.

SUMMARY OF RESULTS

An investigation was conducted in the Lewis 8- by 6-foot supersonic wind tunnel to determine the performance characteristics of twin-duct ram-type side inlets joining into a common duct and mounted on the fuselage forebody of a one-fourth scale model of a supersonic airplane. The tests were conducted at Mach numbers of 1.5 and 1.7 through a range of

2976

CQ-2 back

angles of attack, angles of yaw, and mass-flow ratios. The inlets utilized 6° two-dimensional compression ramps and fuselage boundary-layer-removal systems. Inlet modifications were investigated to determine the effects of (1) side fairings, (2) ramp-support struts, (3) sharp and blunt cowl lips, and (4) a revised area distribution in the subsonic diffuser. The following results were obtained:

1. All the inlet modifications investigated resulted in small changes in the performance characteristics of the blunt-lip inlet with side fairings.

2. At low mass-flow ratios, one inlet operated at a higher mass-flow ratio than the other for all the configurations tested. Lowering the inlet so that part of the ramp was immersed in the boundary layer appreciably decreased the subcritical mass-flow range in which both ducts would operate at the same mass-flow conditions.

3. Increasing the rate of expansion in the subsonic diffuser for the blunt-lip inlet without side fairings increased the critical diffuser total-pressure recovery $1\frac{1}{2}$ percent at a Mach number of 1.5.

4. Neither side fairings nor sharpening of the cowl lips appreciably affected the diffuser total-pressure recovery.

Lewis Flight Propulsion Laboratory
National Advisory Committee for Aeronautics
Cleveland, Ohio, August 21, 1953

2976

REFERENCE

1. Bailey, Neal P.: Thermodynamics of Air at High Velocities. Jour. Aero. Sci., vol. 11, no. 3, July 1944, pp. 227-238.

Figure 1. - Model mounted in tunnel.

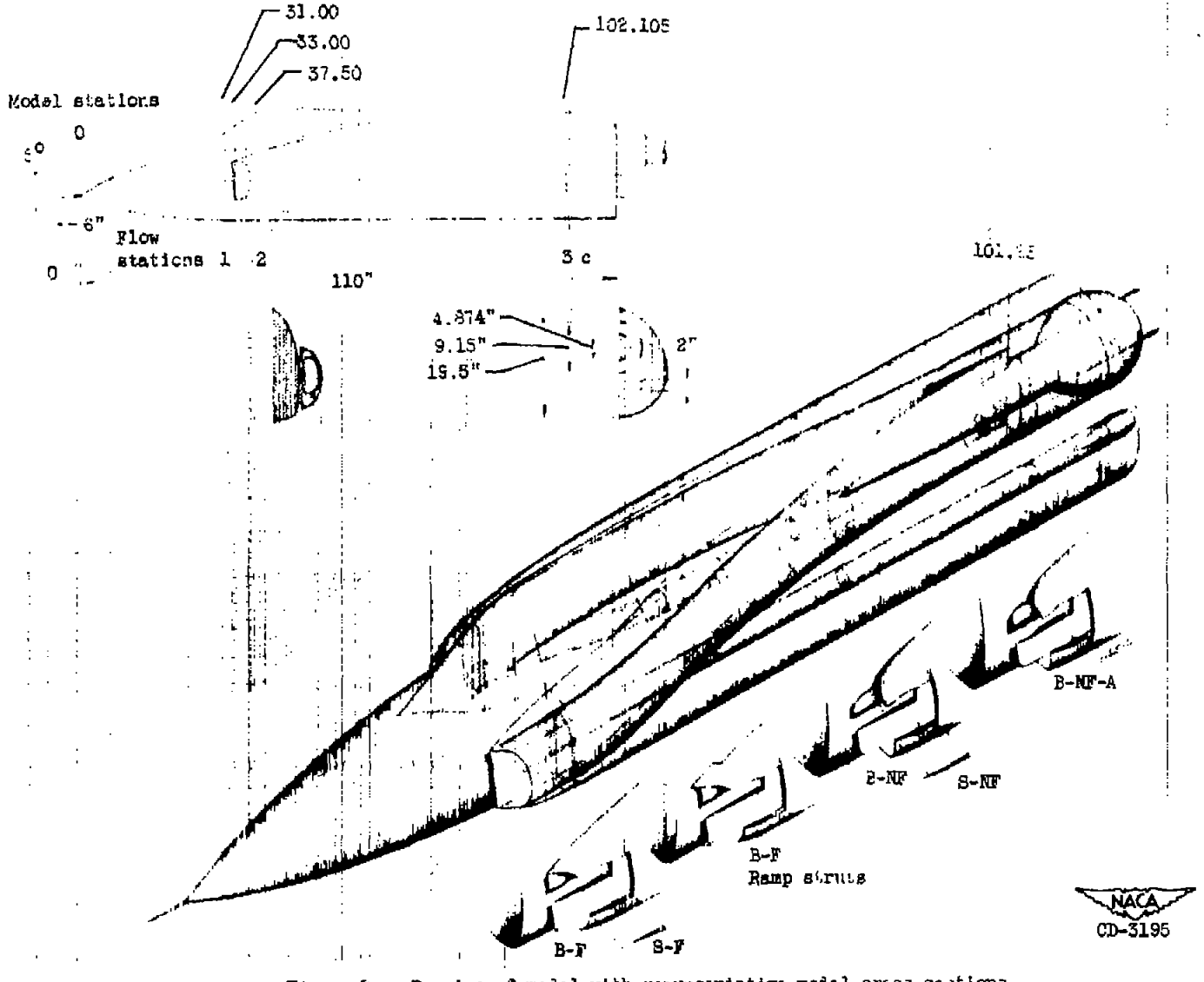

Figure 2. - Drawing of model with representative model cross sections.

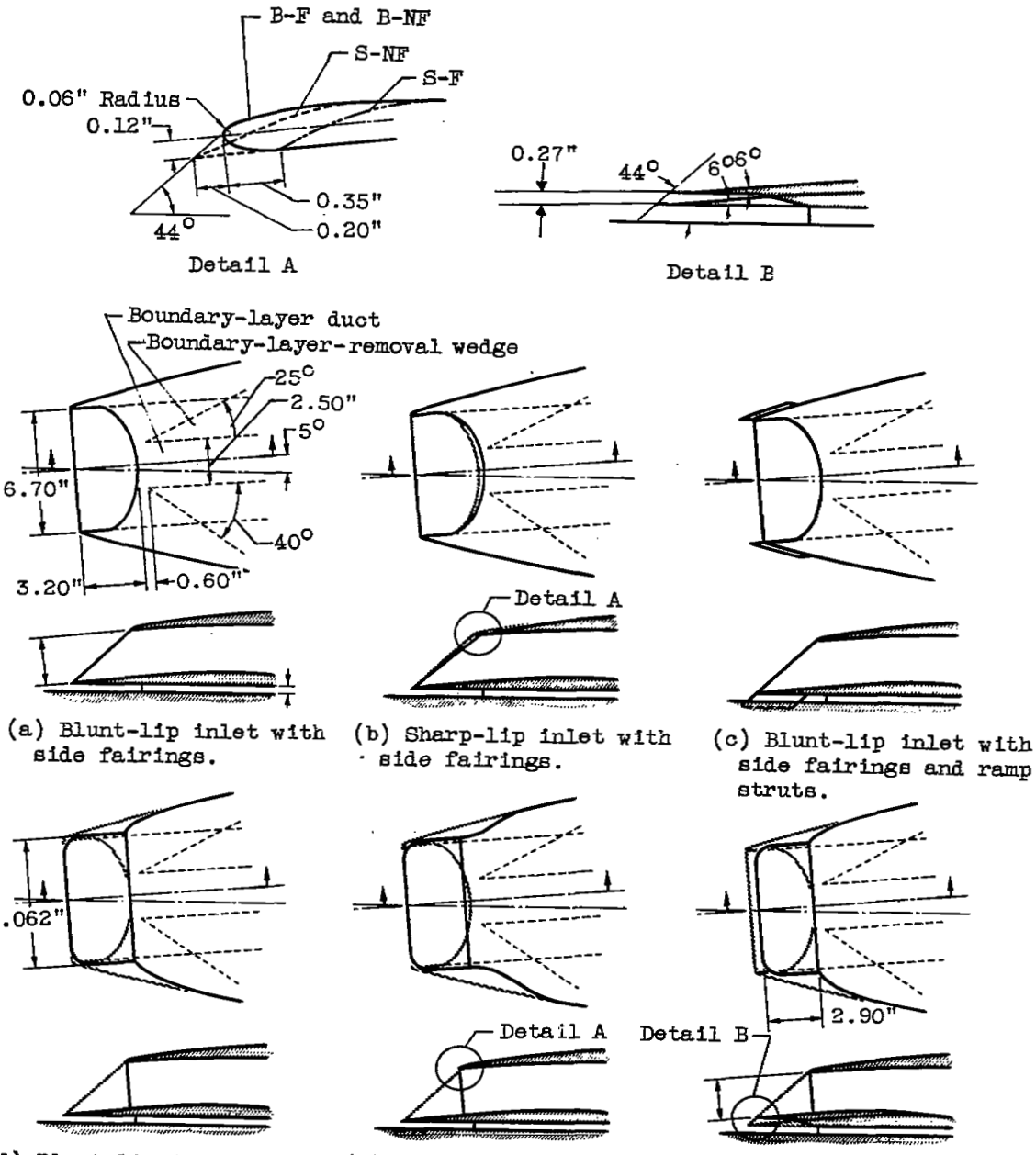

(a) Blunt-lip inlet with side fairings.

(b) Sharp-lip inlet with side fairings.

(c) Blunt-lip inlet with side fairings and ramp struts.

(d) Blunt-lip inlet with no side fairings.

(e) Sharp-lip inlet with nc side fairings.

(f) Blunt-lip inlet with no side fairings. Modified duct area.

Figure 3. - Details of various inlet configurations.

NACA

CD-3196

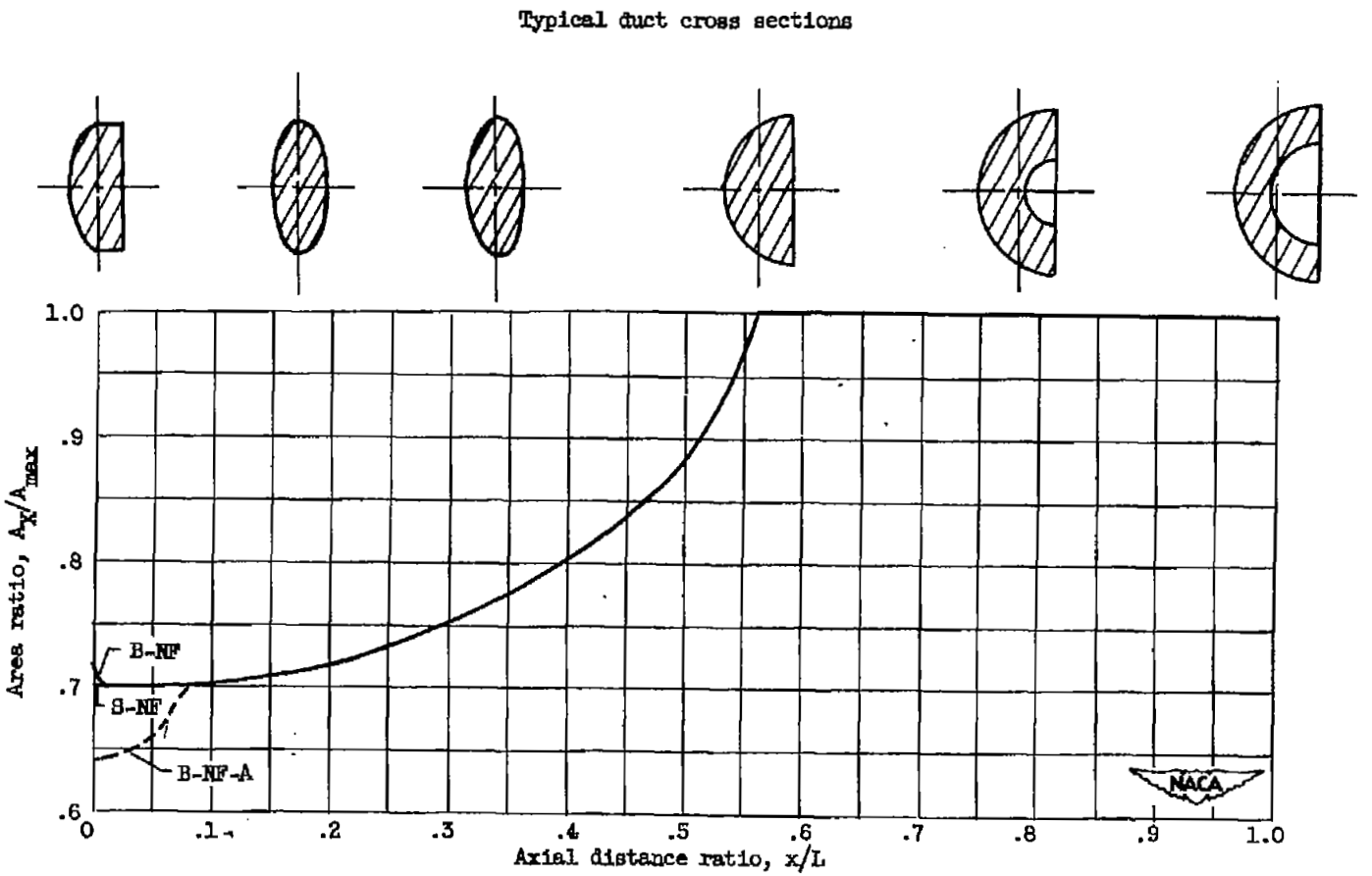

Figure 4. - Subsonic-diffuser area variation.

2976

CQ-3

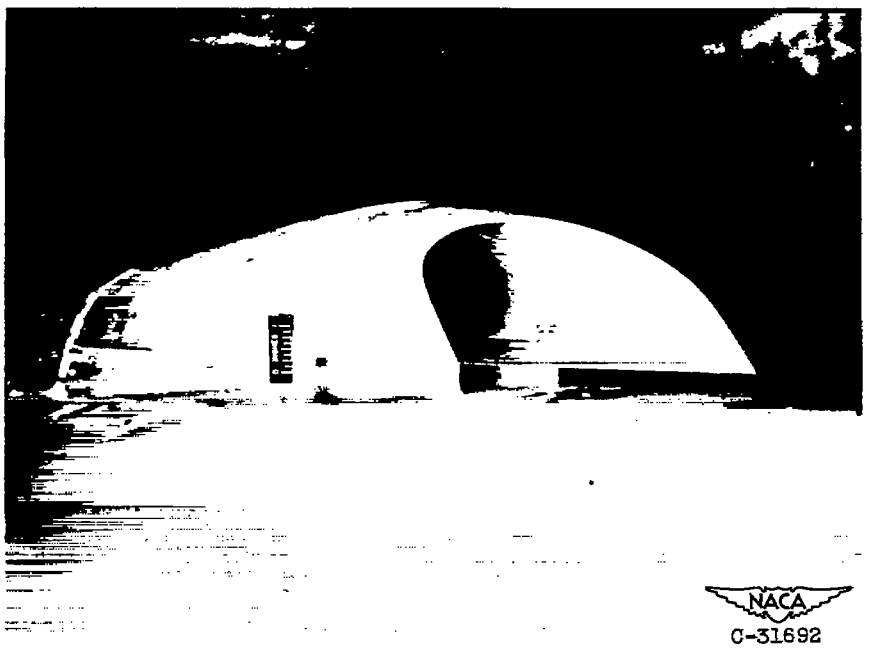

(a) Blunt-lip inlet with side fairings.

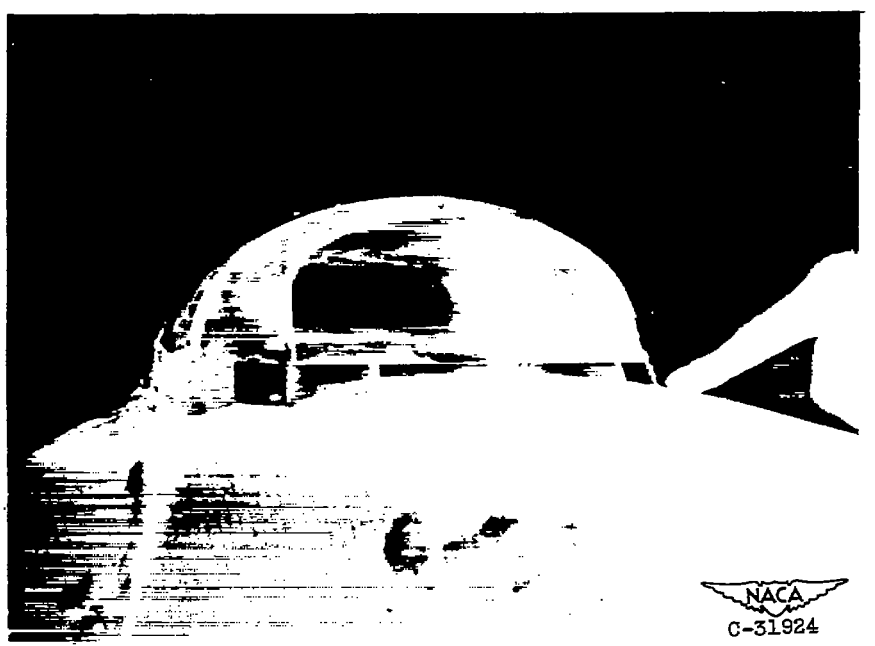

(b) Blunt-lip inlet with side fairings and ramp struts.

Figure 5. - Inlet configurations.

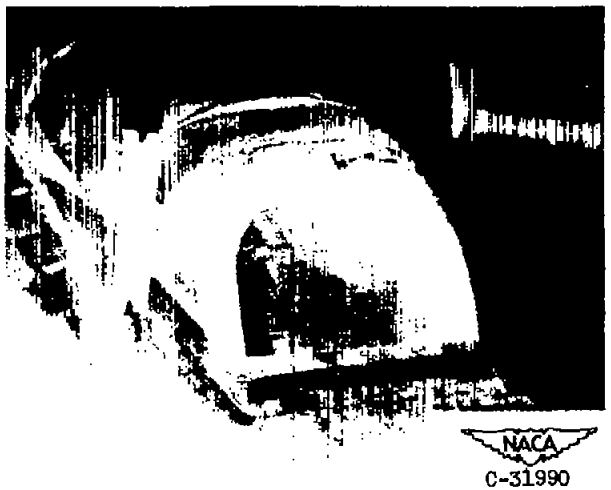

(c) Sharp-lip inlet with side fairings.

(d) Blunt-lip inlet with no side fairings.

(e) Sharp-lip inlet with no side fairings.

Figure 5. - Concluded. Inlet configurations.

Angle of attack, α, deg	Free-stream Mach number, M_0			
	1.5		1.7	
	Average inlet Mach number, $M_{i,av}$	Average inlet flow deflection, $\beta_{i,av}$, deg	Average inlet Mach number, $M_{i,av}$	Average inlet flow deflection, $\beta_{i,av}$, deg
9.5	-----	---	1.71	7.5
5	1.495	0.3	1.70	0.3
1.5	-----	---	1.71	-6.2

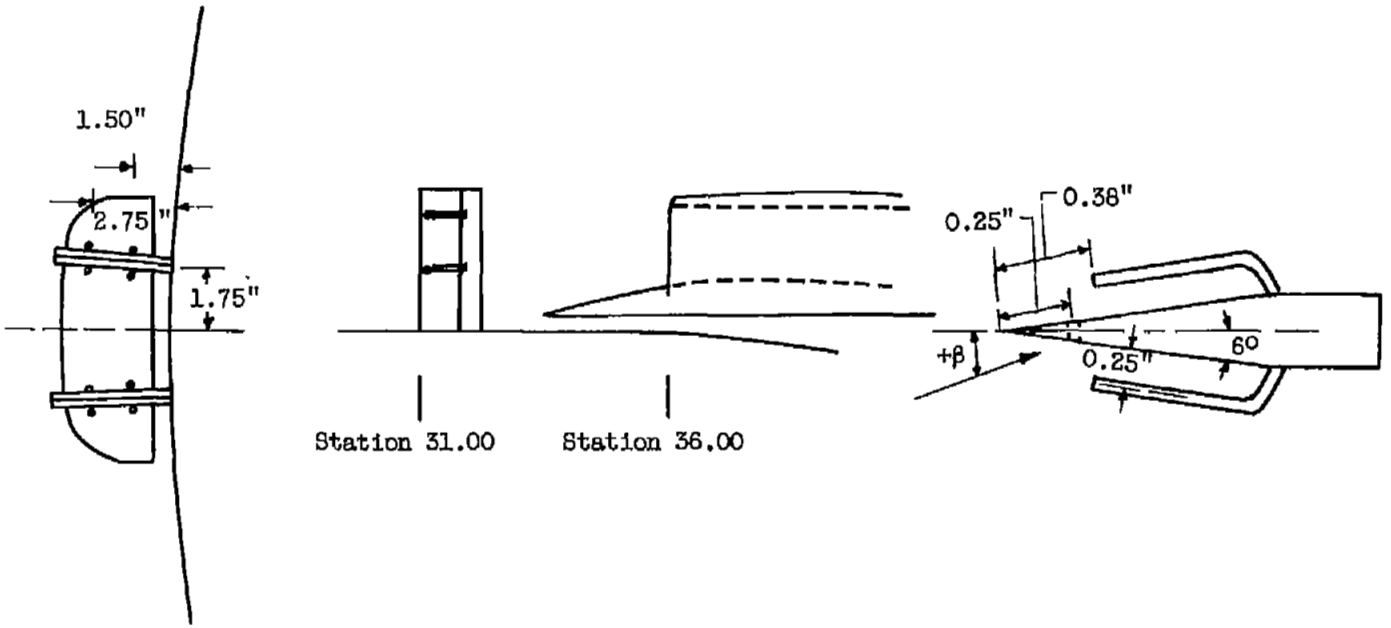

Figure 6. - Details of wedges and survey results.

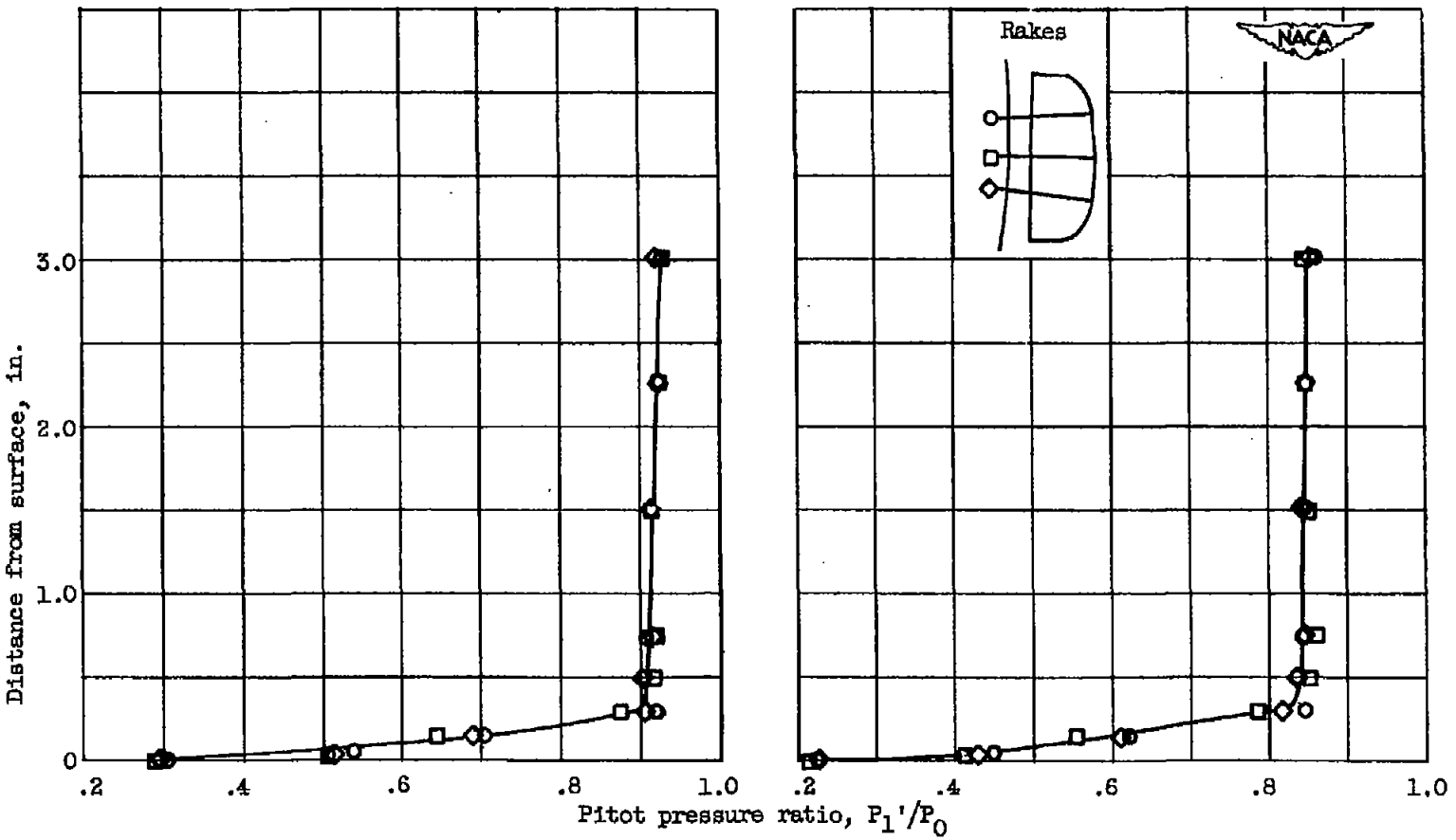

(a) Mach number, 1.5. (b) Mach number, 1.7.

Figure 7. - Boundary-layer profiles ahead of inlet at angle of attack of 5°.

2976

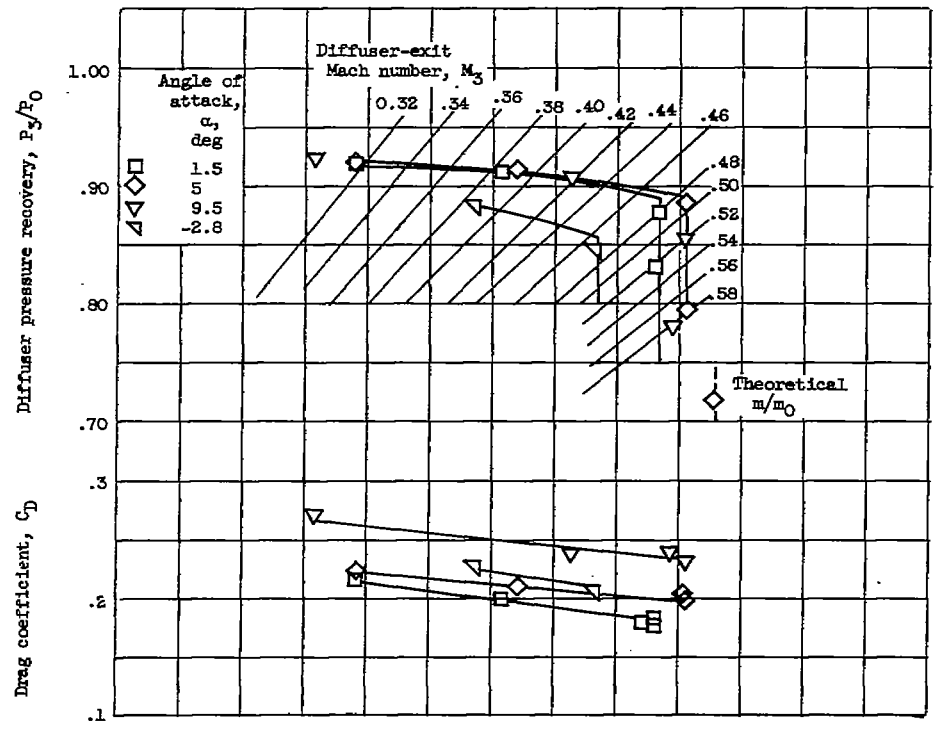

(a) Mach number, 1.5.

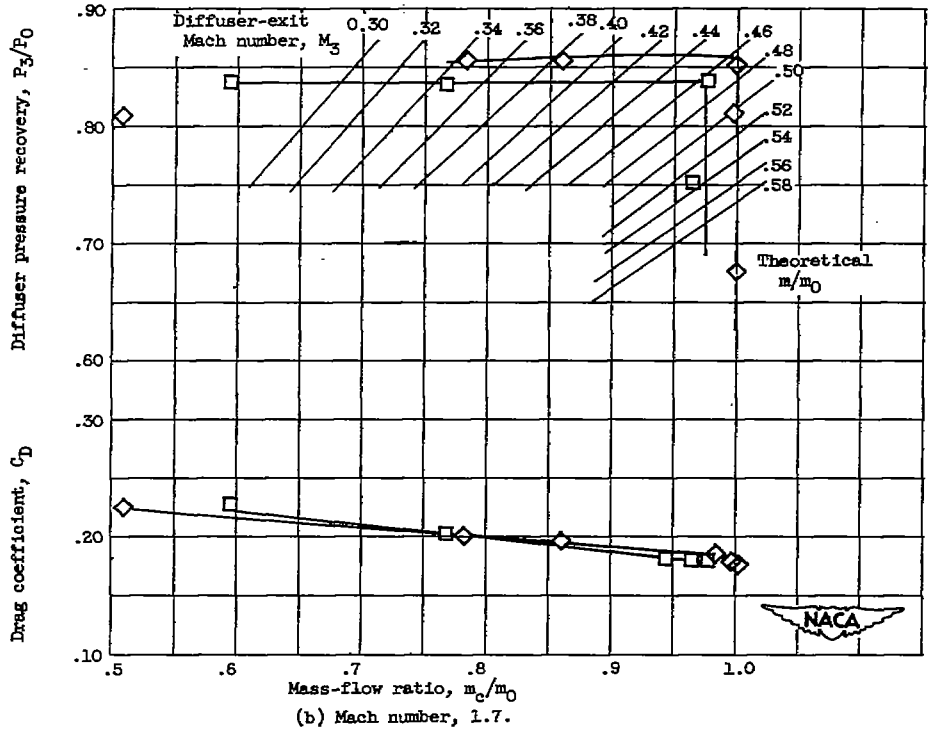

(b) Mach number, 1.7.

Figure 8. - Performance characteristics of inlet B-F.

[redacted]

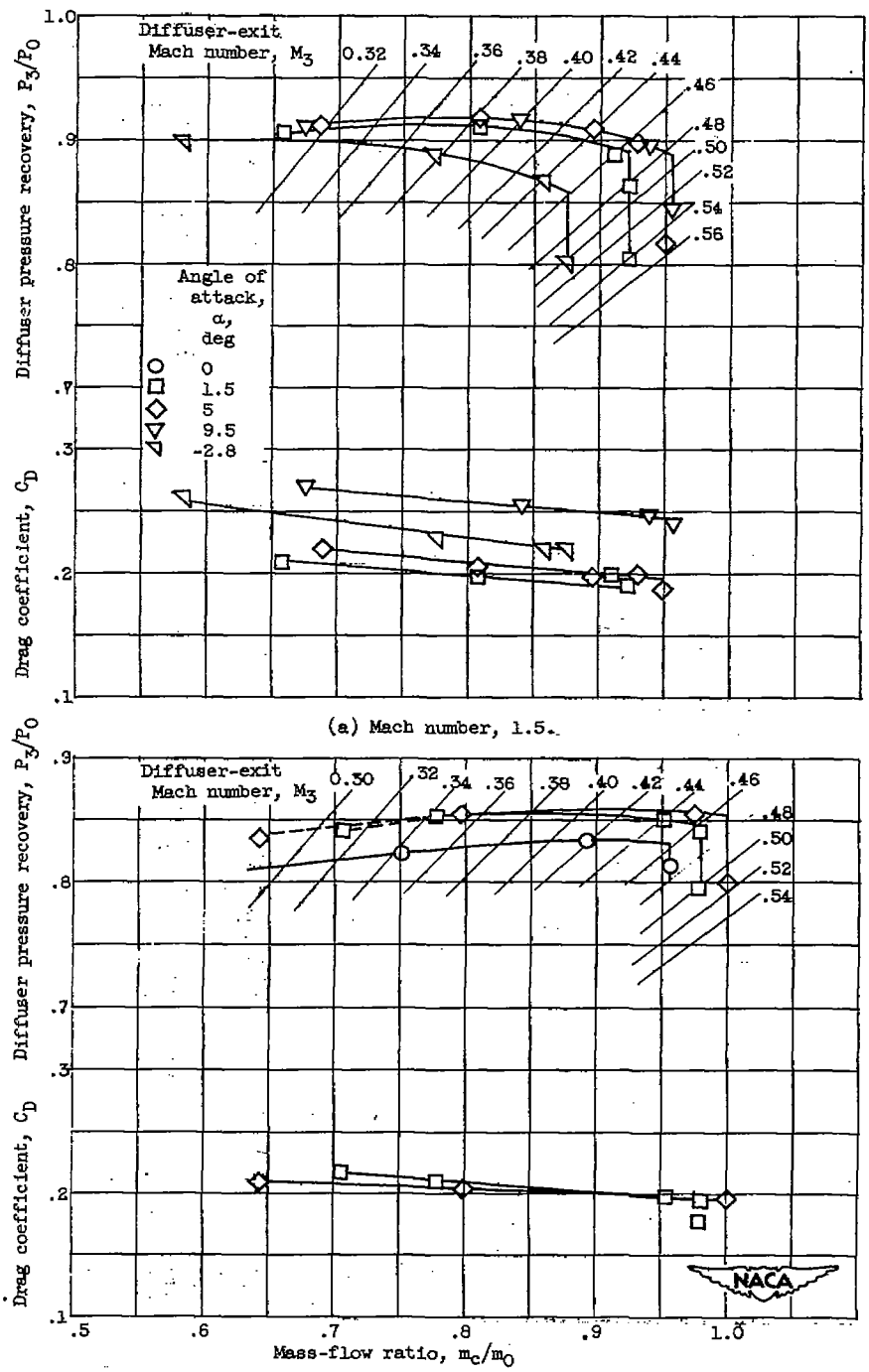

(a) Mach number, 1.5.

(b) Mach number, 1.7.

Figure 9. - Performance characteristics of inlet B-NF.

[redacted]

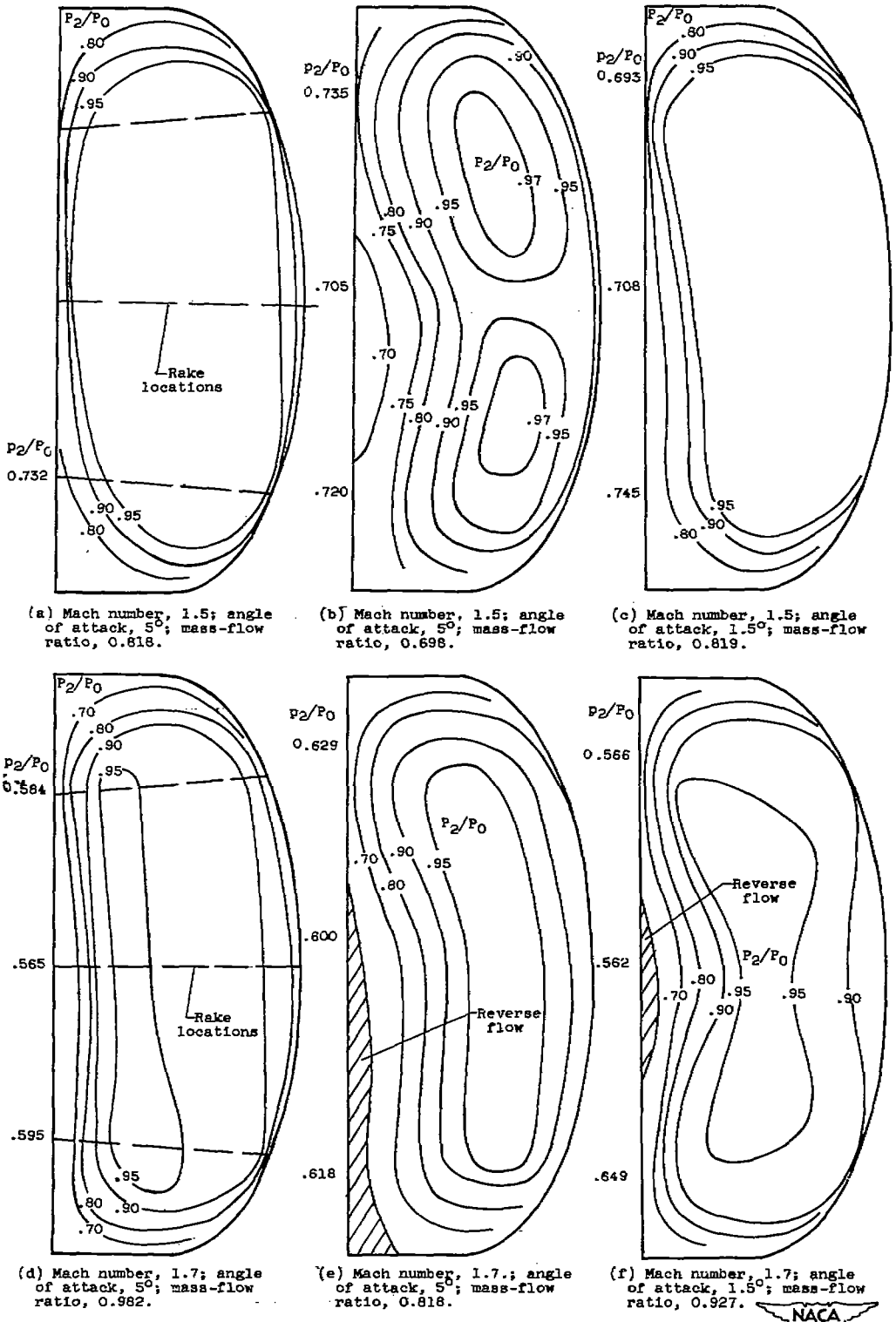

(a) Mach number, 1.5; angle of attack, 5°; mass-flow ratio, 0.818.

(b) Mach number, 1.5; angle of attack, 5°; mass-flow ratio, 0.698.

(c) Mach number, 1.5; angle of attack, 1.5°; mass-flow ratio, 0.819.

(d) Mach number, 1.7; angle of attack, 5°; mass-flow ratio, 0.982.

(e) Mach number, 1.7; angle of attack, 5°; mass-flow ratio, 0.818.

(f) Mach number, 1.7; angle of attack, 1.5°; mass-flow ratio, 0.927.

Figure 10. - Contours of total-pressure recovery P_2/P_0 for inlet B-NF.

[redacted]

2976

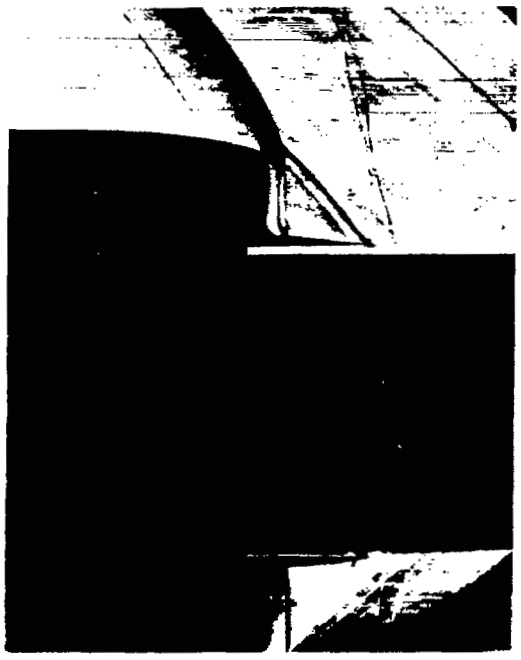

(a) Mach number, 1.5; mass-flow ratio, 0.909.

(b) Mach number, 1.5; mass-flow ratio, 0.801.

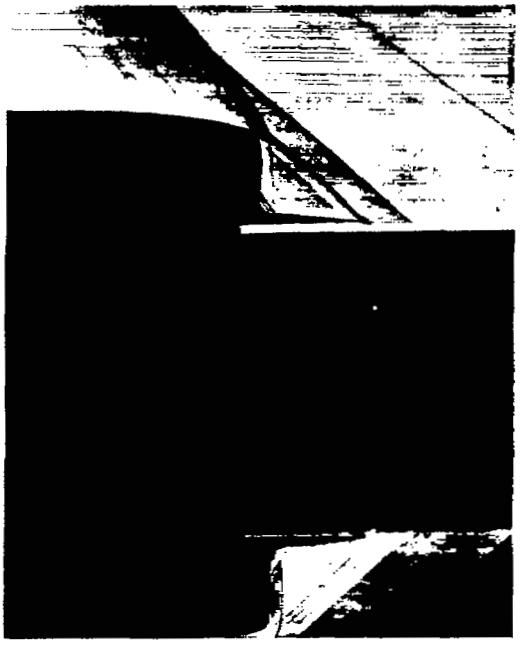

(c) Mach number, 1.7; mass-flow ratio, 0.957.

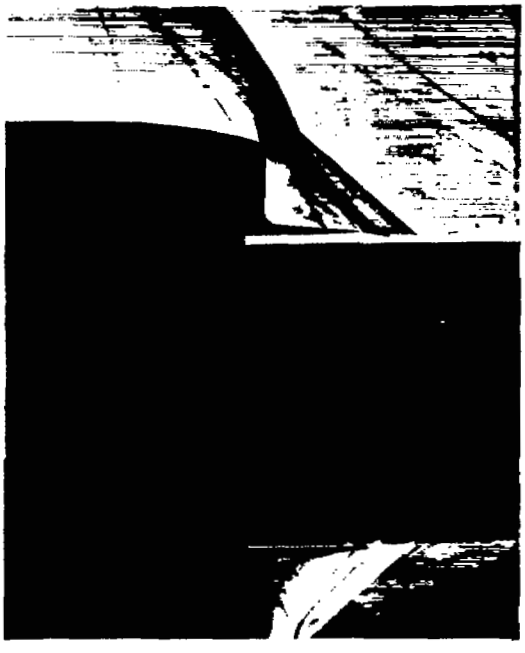

(d) Mach number, 1.7; mass-flow ratio, 0.752.

NACA C-33406

Figure 11. - Schlieren photographs for inlet B-NF.

2976

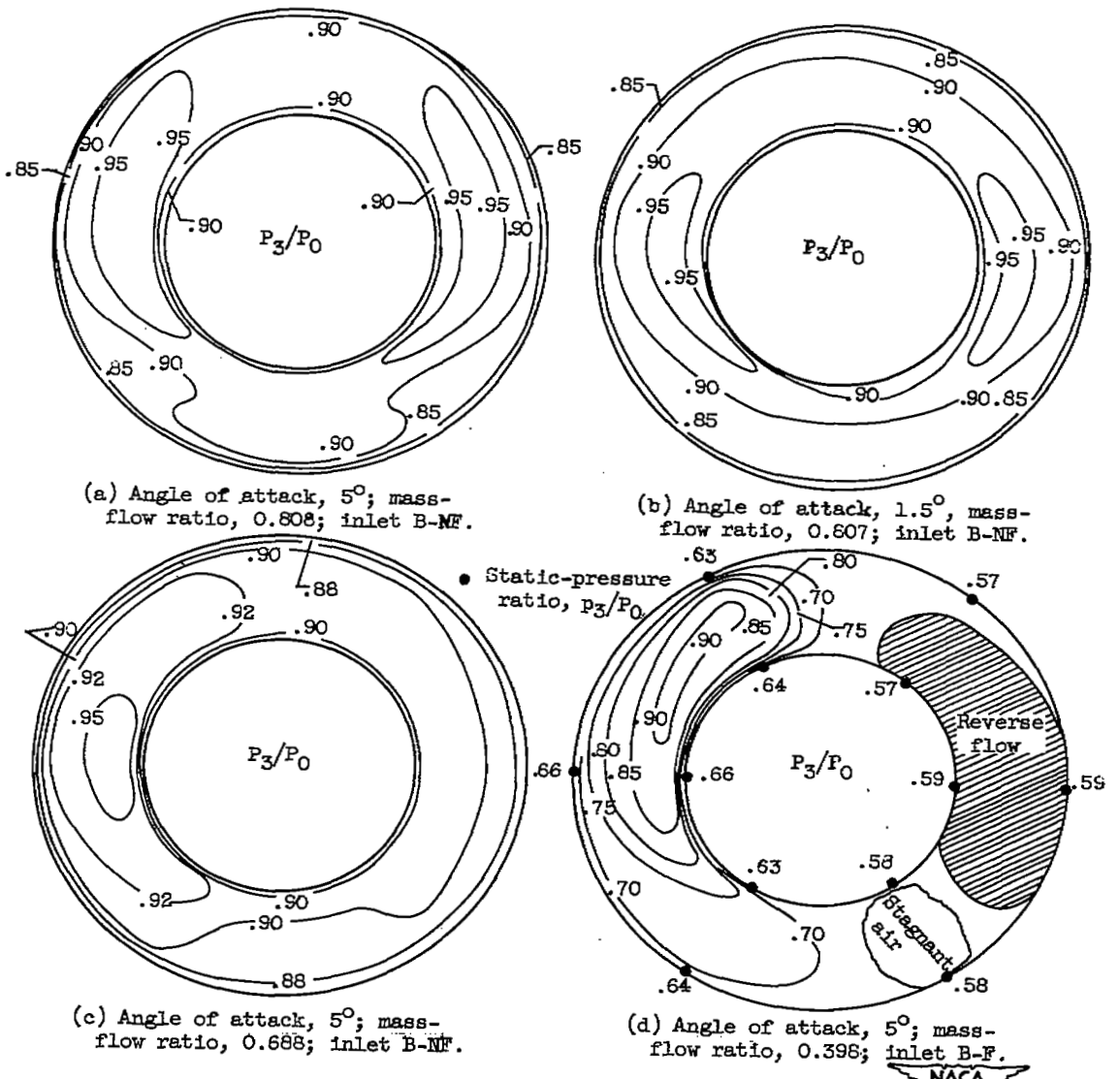

(a) Angle of attack, 5°; mass-flow ratio, 0.808; inlet B-NF.

(b) Angle of attack, 1.5°, mass-flow ratio, 0.807; inlet B-NF.

(c) Angle of attack, 5°; mass-flow ratio, 0.688; inlet B-NF.

(d) Angle of attack, 5°; mass-flow ratio, 0.398; inlet B-F.

Figure 12. - Contours of diffuser-exit total-pressure recovery P_3/P_0 at Mach number of 1.5 for inlets B-NF and B-F.

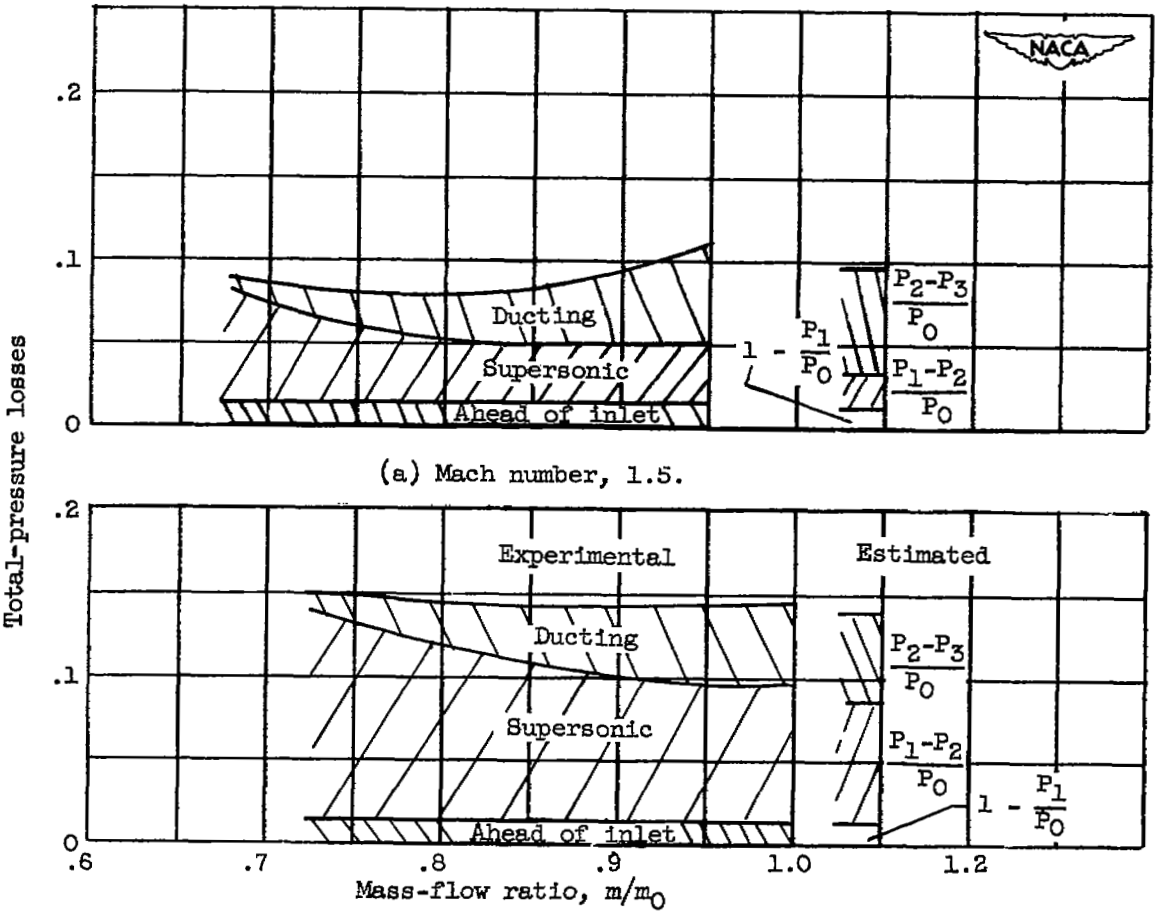

(a) Mach number, 1.5.

(b) Mach number, 1.7.

Figure 13. - Breakdown of total-pressure losses for inlet B-NF at angle of attack of 5°.

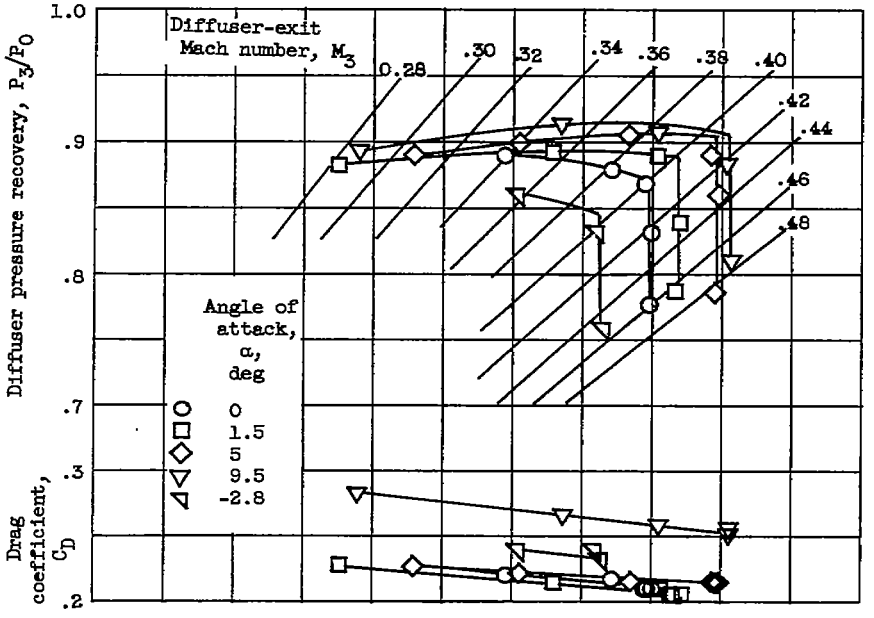

(a) Mach number, 1.5.

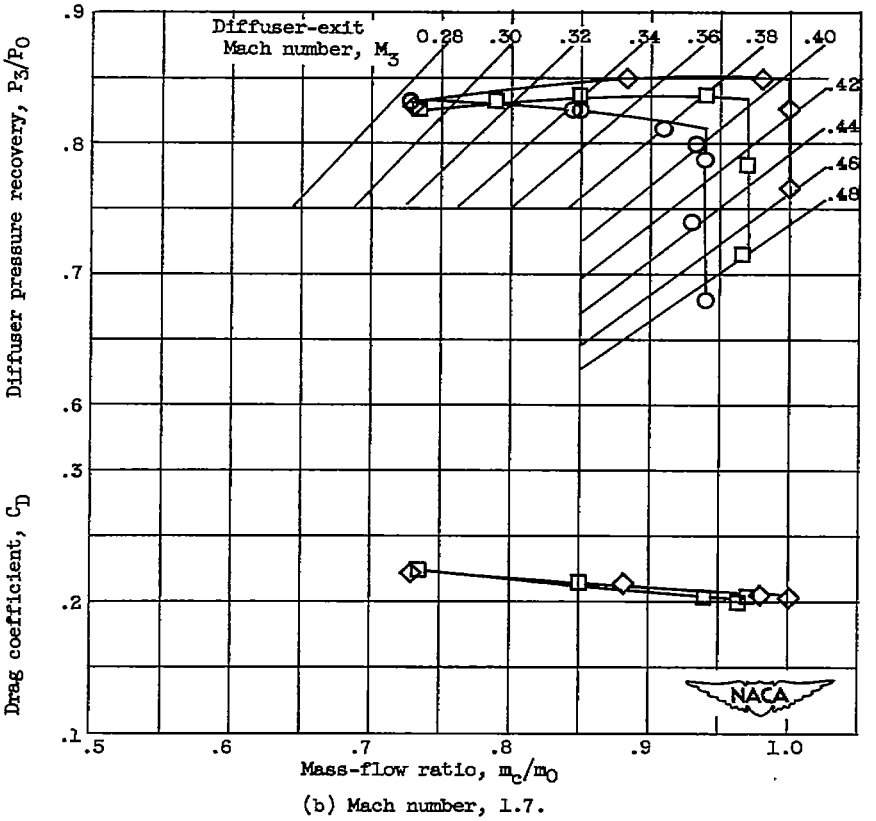

(b) Mach number, 1.7.

Figure 14. - Performance characteristics of inlet B-NF-A.

[redacted]

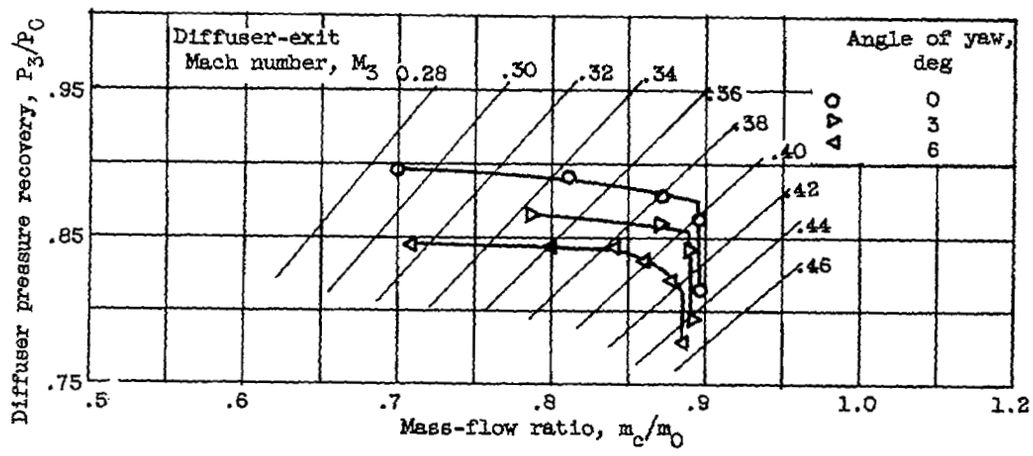

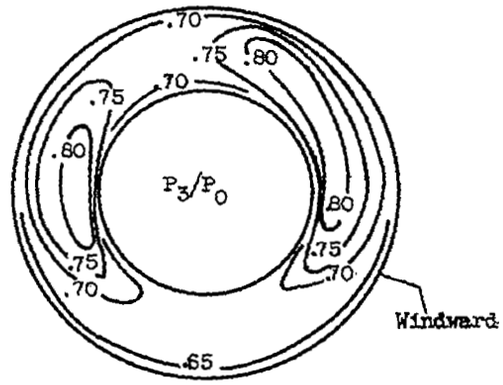

(a) Angle of yaw, 3°; mass-flow ratio, 0.890.

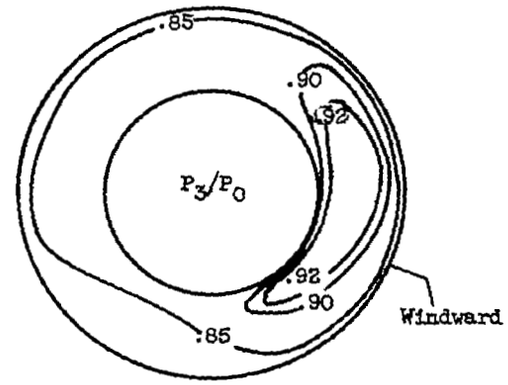

(b) Angle of yaw, 3°; mass-flow ratio, 0.785.

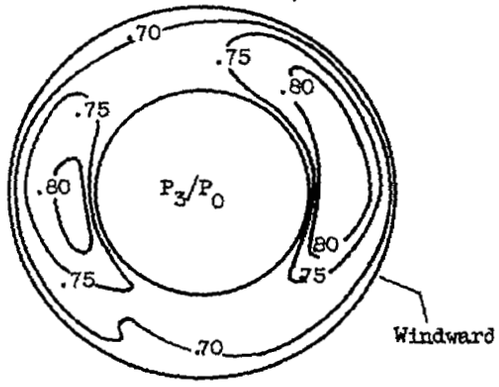

(c) Angle of yaw, 6°; mass-flow ratio, 0.885.

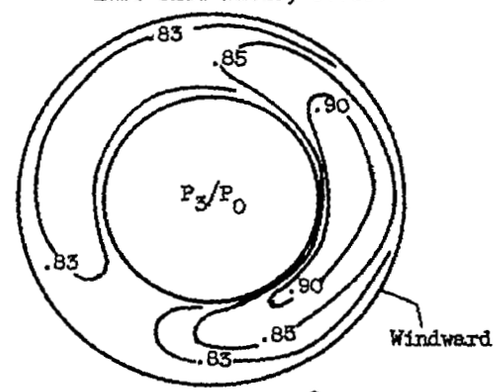

(d) Angle of yaw, 6°; mass-flow ratio, 0.800.

Figure 15. - Performance characteristics of inlet B-NF-A and diffuser-exit total-pressure contours P_3/P_0 for Mach number 1.5.

[redacted]

2976

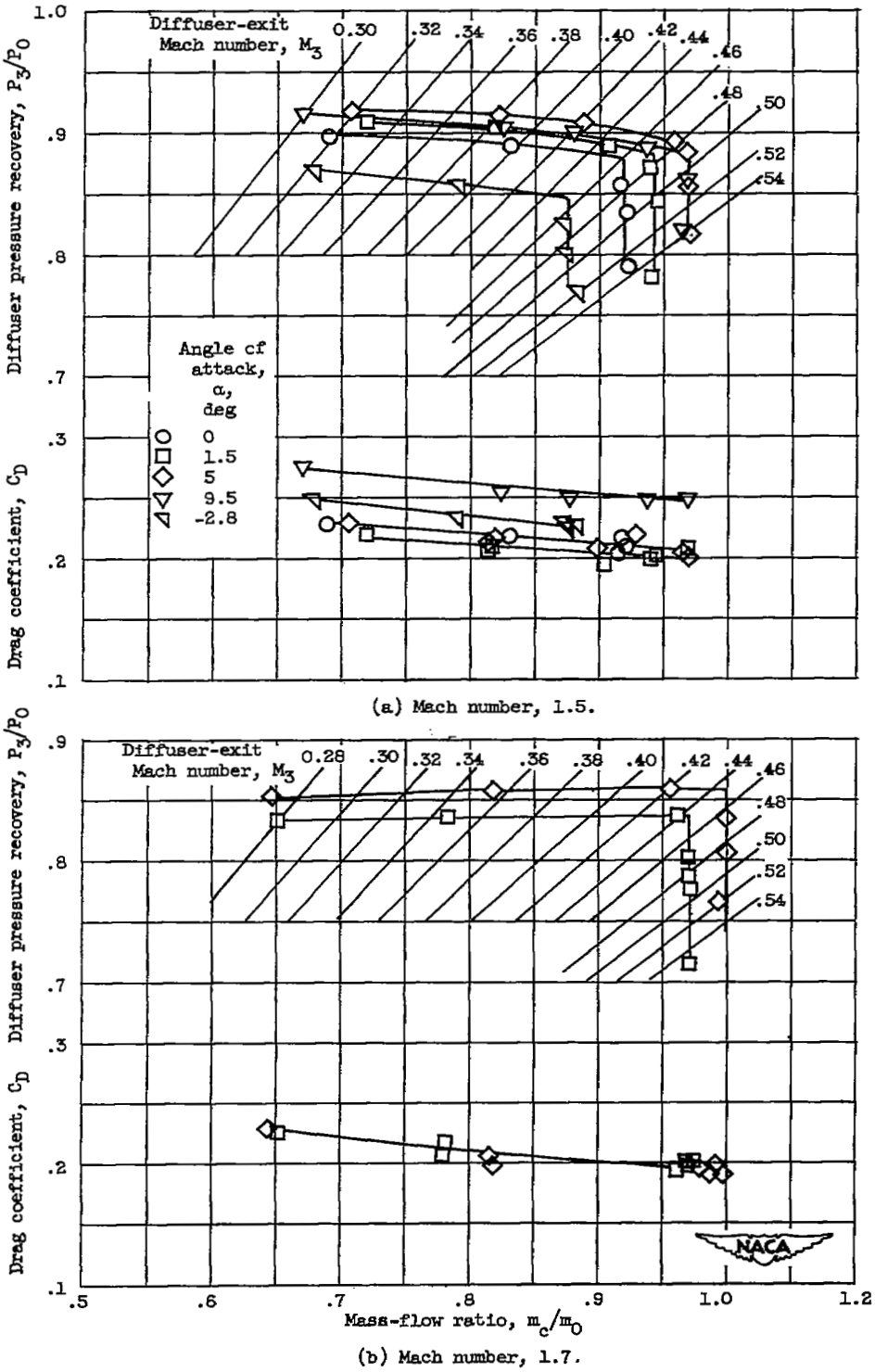

(a) Mach number, 1.5.

(b) Mach number, 1.7.

Figure 16. - Performance characteristics of inlet S-F.

[redacted]

NACA-Langley - 10-12-53 - 325

SECURITY INFORMATION